

**Development of historical forest attribute layers using
Landsat time series and kNN imputation for the western
Canadian boreal forest**

A report prepared for the LandWeb project

Prepared by:

Paul D. Pickell
Nicholas C. Coops
University of British Columbia
Vancouver, B.C.
December 2016

For inquiries: paul.pickell@forestry.ubc.ca

Summary

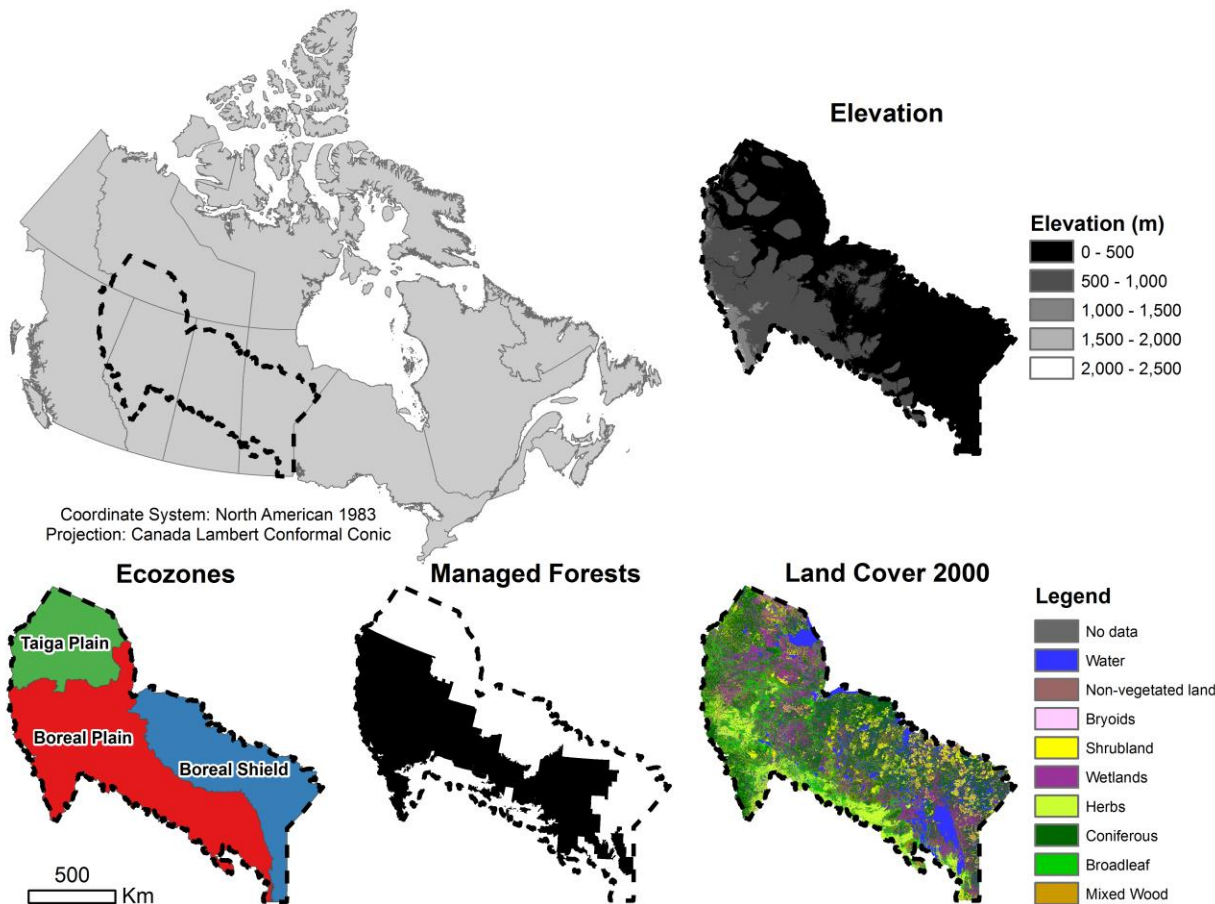
The purpose of this report is to describe the creation of spatially continuous layers of forest attributes for the LandWeb study area. A primary objective of the LandWeb project is the prediction of forest attributes (height, canopy cover, and species) for the years 1990, 2000, 2010, and a dateless layer. These layers are designed to assist modelers in back-casting the LandWeb study area to the pre-industrial landscape condition.

In this technical note, we describe the methods for predicting the target forest attributes across the LandWeb study area using a k-nearest neighbor (kNN) approach. We utilized the Common Attribute Schema for Forest Resource Inventories (CASFRI) dataset for training a kNN model and acquired several ancillary datasets to impute the target forest attributes for locations of the LandWeb study area where CASFRI data were not available. We cross-validated the predicted attributes with a reserved set of the observed CASFRI records to derive estimates of accuracy. Accuracy statements for the layers are provided to support and we discuss the possible uses for the predictions.

LandWeb Study Area

The LandWeb study area encompasses more than 208 Mha of the western Canadian boreal forest, extending between approximately 48°58'N to 65°6'N latitude and 92°0'W to 127°6'W longitude (Figure 1). The region covers a large elevation gradient extending from the continental shield (<500 m) to the foothills of the Rocky Mountains (>2000 m). Four distinct ecozones are recognized within the study area, namely subdivisions of plains and shield boreal ecosystems (ESWG 1996). Approximately 40% of the forested ecosystems are actively managed or tenured for wood fiber production, which is primarily limited to the southern extent of the study area. The land cover in 2000 is variable across the study area, with most forested ecosystems dominated by coniferous species or mixedwood stand associations (Wulder et al. 2003).

Figure 1. LandWeb study area. Elevation data come from the Advanced Spaceborne Thermal Emission and Reflection Radiometer. Ecozones come from the Ecological Stratification Working Group (1996). Managed forests comes from the Canadian Forest Service. Land cover comes from the 2000 classification of Earth Observation for Sustainable Development of Forests.



Materials and Methods

The k nearest neighbors (kNN) imputation approach

The spatial coverage of forest inventory datasets is often incomplete or limited. In such situations, imputing target attributes like forest height is a common approach for extending those datasets to areas where forest inventory data is not readily available. The *k* nearest neighbors (kNN) technique is a non-parametric, multivariate imputation procedure. The objective of kNN is to find the *k* reference observations that are most similar in a multivariate feature space of predictor variables (*X*) in order to impute the response variable (*Y*) in a location where the response variable is not known, but a set of predictor variables are known. For example, forest height may be available for managed forests, but to extend that attribute to unmanaged forests would require one or more predictor variables that are associated with forest height and that are spatially comprehensive in both managed and unmanaged forests. The imputed value for a target location is simply the average of the response variable for the *k* reference observations. The kNN technique has been widely popularized in forestry applications due to the relatively intuitive and simple computation and desirable statistical properties (McRoberts 2012; Beaudoin et al. 2014).

Forest inventory data and target forest attributes

A set of forest inventory data were derived from the Common Attribute Schema for Forest Inventory (CASFRI) for the study area (Cumming et al. 2015). The CASFRI data included a number of forest attributes derived from various forest inventories from managed forests within the LandWeb study area and were standardized to a common attribute scheme (Cumming et al. 2015). The spatial data were defined as centroids derived from the polygons that were originally interpreted in the aerial forest inventory datasets. The photo year associated with each record was used to segment the CASFRI data into three nominal decades: 1990 (photo year 1989-1991); 2000 (1999-2001); and 2010 (2009-2011).

We selected three target forest attributes as response variables (*Y*) to predict for the LandWeb study area: species association, stand height, and canopy closure. We identified all of the major species associations (*i.e.*, leading species and secondary species), representing 99.8% of all species associations in the CASFRI dataset (Table 1). The high abundance of relatively rare species associations posed a modelling challenge for accurately predicting the species association classes. Our solution was a series of expert consultations within the LandWeb team to reduce these initial 25 associations to 13 final species associations (Table 1). Height and canopy cover were represented by upper and lower limits in the CASFRI dataset. We averaged these limits to derive the estimate of stand height and canopy cover. The codes associated with each predicted data layer are provided in Table 2.

CASFRI records were excluded if they had incomplete information about the three target forest attributes or lacked photo year information or represented an area smaller than 1 ha. We also excluded CASFRI records if they were disturbed within one year of the photo year or if the estimated height was less than 4 m. Analysis of autocorrelograms for stand height and canopy cover indicated that spatial autocorrelation was negligible beyond 3 km, so the CASFRI data were randomly sampled at this distance for height and canopy cover. CASFRI samples from all

decades were pooled together to train the kNN model using the predictor variables described in the next section.

Samples for species associations were not limited by the 3 km threshold in the final sample selection due to many fewer samples available for the 13 species association classes. Moreover, the distribution of species associations across the available CASFRI data was highly imbalanced. For example, Pure Deciduous composed nearly a third of all CASFRI records (Table 1). Therefore, we made an effort to balance the representation of the 13 species associations in the random sampling procedure by imposing a target sample of $n=500$ for each species association class. The sampling rules described above for the decades were applied to the dateless predictions of the forest attributes. All available CASFRI records from any year were utilized in the dateless kNN model training. Due to the larger number of available samples in the species associations, the target sample size was increased to $n=1,000$ for each of the 13 species associations.

Table 1. Top 25 species associations representing 99.8% of all CASFRI records. All non-conifer deciduous species were collapsed into a Deciduous class and all pines were collapsed into a Pinus class. The first column designates the top 5 species ranked by abundance in the CASFRI dataset. The rank columns refer to the top 5 secondary species observed for a given leading species. Values in parentheses show the percentage of CASFRI records represented by a leading species or the ranked species association. Pure associations were defined as leading species $\geq 80\%$ by cover. Colored species associations refer to associations that were grouped by expert opinion.

Leading Species (% CASFRI)	Rank 1	Rank 2	Rank 3	Rank 4	Rank 5
Deciduous (42.9)	Pure (31.5)	Pice glau (7.2)	Pinus (3.1)	Pice mari (1.2)	Lari lari (<1)
Pice mari (26.5)	Pure (10.1)	Lari lari (7.0)	Pinus (5.4)	Pice glau (2.1)	Deciduous (1.9)
Pinus (16.4)	Pice mari (6.0)	Deciduous (4.5)	Pure (3.5)	Pice glau (2.4)	Lari lari (<1)
Pice glau (10.0)	Deciduous (5.2)	Pure (2.1)	Pinus (1.4)	Pice mari (1.3)	Lari lari (<1)
Lari lari (4.0)	Pice mari (2.8)	Pure (1.1)	Deciduous (<1)	Pice glau (<1)	Pinus (<1)

Selection of predictor variables

A total set of 23 predictor variables (X) were acquired as geo-spatial layers for the study area. This set included 14 spectral variables derived from composite Landsat satellite imagery, 8 climate variables derived from ClimateNA (Hamann et al. 2013), and a digital elevation model (DEM) derived from the Advanced Spaceborne Thermal Emission and Reflection Radiometer (ASTER) sensor aboard the Terra satellite (Table 3).

Landsat imagery during the growing season were downloaded directly from United States Geological Survey Earth Resources Observation and Science Center as Level 1 surface reflectance products (Masek et al. 2006), which are systematically corrected for radiometric and geometric accuracy. Composite Landsat images at a spatial resolution of 30 m for 1990, 2000, and 2010 were generated using best-available pixel (BAP) criteria described in White et al. (2013) in order to reduce data gaps caused by clouds, cloud shadows, and haze. Even with the BAP compositing procedure, there were still some persistent data gaps for which a best available pixel was unavailable. In addition to the 6 spectral bands of the Landsat imagery, we derived 5 commonly computed spectral indices (Table 3). The Tasseled Cap components (brightness,

greenness, wetness) were also averaged over a local 3x3 pixel window to provide a neighborhood spectral metric in the prediction.

The climate variables were derived from the ClimateNA software package (v5.10) at a spatial resolution of 1 km for the study area (Hamann et al. 2013). From 23 candidate climate variables, we retained 8 variables (Table 3). All geo-spatial layers were re-projected to the Lambert Conformal Conic projection (North American Datum 1983) and resampled to the target resolution of 100 m using cubic interpolation. Each X variable was normalized to a standard score using the following equation:

$$X\text{-}norm = \frac{x - \sigma}{\mu}$$

Table 2. Code values of predicted data layers.

Variable	Code	Value
Height (m)	5 - 27	Height in meters
Canopy cover (%)	5 - 90	Canopy cover in percentage
Species associations*	11 14 22 23 26 31 32 33 34 41 42 43 44 201	Deciduous pure Deciduous, Pice glau Pice mari pure Pice mari, Pinus Pice mari, other Pinus, Deciduous Pinus, Pice mari Pinus pure Pinus, Pice glau Pice glau, Deciduous Pice glau, Pice mari Pice glau, Pinus Pice glau pue Tie in the prediction
Codes common to all data layers	200 210 220 230 240 255	No data Anthropogenic footprint Water Non-vegetated Vegetated, non-forested Outside of study area

* For non-pure species associations, defined as less than 80% cover by the leading species in the CASFRI dataset, the leading species is given first followed by the secondary species.

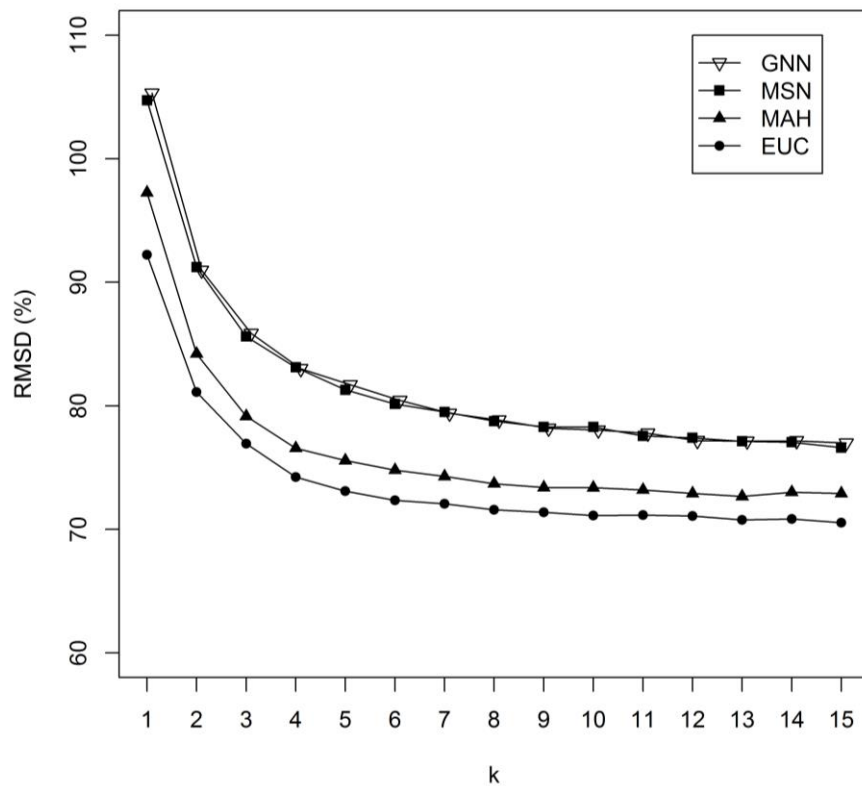
Table 3. Summary of predictor variables used in the study.

Variable name	Formulation or description	Acronym	Units	Spatial resolution
Landsat band 1	Visible blue	B1	--	30 m
Landsat band 2	Visible green	B2	--	30 m
Landsat band 3	Visible red	B3	--	30 m
Landsat band 4	Near-infrared	B4	--	30 m
Landsat band 5	Mid-infrared	B5	--	30 m
Landsat band 7	Mid-infrared	B7	--	30 m
Normalized differenced vegetation index	$\frac{\text{Band 4} - \text{Band 3}}{\text{Band 4} + \text{Band 3}}$	NDVI	--	30 m
Normalized burn ratio	$\frac{\text{Band 4} - \text{Band 6}}{\text{Band 4} + \text{Band 6}}$	NBR	--	30 m
Normalized differenced built-up index	$\frac{\text{Band 5} - \text{Band 4}}{\text{Band 5} + \text{Band 4}}$	NDBI	--	30 m
Tasselled Cap brightness	$(\text{Band 1} * 0.3561) + (\text{Band 2} * 0.3972) + (\text{Band 3} * 0.3904) + (\text{Band 4} * 0.6966) + (\text{Band 5} * 0.2286) + (\text{Band 7} * 0.1596)$	TCB	--	30 m
Tasselled Cap greenness	$(-0.3344 * \text{Band 1}) + (-0.3544 * \text{Band 2}) + (-0.4556 * \text{Band 3}) + (\text{Band 4} * 0.6966) + (-0.0242 * \text{Band 5}) + (-0.2630 * \text{Band 7})$	TCG	--	30 m
Tasselled Cap wetness	$(\text{Band 1} * 0.2626) + (\text{Band 2} * 0.2141) + (\text{Band 3} * 0.0926) + (\text{Band 4} * 0.0656) + (-0.7629 * \text{Band 5}) + (-0.5388 * \text{Band 7})$	TCW	--	30 m
Mean annual temperature	Mean annual temperature between 1961-1990	MAT	°C	1,000 m
Temperature difference	Mean warmest month – Mean coldest month	TD	°C	1,000 m
Mean annual precipitation	Mean annual precipitation between 1961-1990	MAP	mm	1,000 m
Summer heat-moisture index	$\frac{\text{Mean warmest month temperature}}{\text{May to September Precipitation / 1000}}$	SHM	--	1,000 m
Precipitation as snow	Mean annual snowfall August-July between 1961-1990	PAS	mm	1,000 m
Extreme minimum temperature	Minimum annual temperature between 1961-1990	EMT	°C	1,000 m
Extreme maximum temperature	Maximum annual temperature between 1961-1990	EXT	°C	1,000 m
Relative humidity	Mean annual relative humidity between 1961-1990	RH	%	1,000 m
Digital elevation model	ASTER	DEM	m	30 m

Optimization of kNN parameters and implementation

The kNN analysis requires that the number of nearest neighbors be considered prior to undertaking the prediction (McRoberts et al. 2012). Ideally, the number of k neighbors should be high to derive an accurate prediction, but in practice this value is limited by computational efficiency since additional k nearest neighbors each raise the number of computations by one power. A common method for deriving the value of k is comparing the root mean squared difference (RMSD%) using a reference and validation set of the data while varying the value of k . We also tested four commonly used distance metrics: Euclidean (EUC); Mahalanobis (MAH); gradient nearest neighbor (GNN); and most similar neighbor (MSN). For each distance metric, reference-validation sets were replicated 1,000 times and imputed for both stand height and canopy cover, with RMSD% computed for values of k ranging from 1 to 15. We used the Euclidean distance metric and selected $k=15$ as a compromise between having sufficient reference neighbors to distinguish 13 species association classes while minimizing the number of computations.

Figure 2. Root mean squared difference percentage as a function of increasing k nearest neighbors. Three commonly-used distance metrics are shown: Euclidean (EUC); Mahalanobis (MAH); gradient nearest neighbor (GNN); and most similar neighbor (MSN).



The implementation of the kNN procedure was undertaken in a multi-phase process. The exact nearest neighbors were computed using the Approximate Nearest Neighbors (ANN) function of

the *yaImpute* package in R (Crookston and Finley 2008). The ANN function provided the fastest search for the 15 nearest neighbors from the thousands of total reference observations that we were able to achieve in our testing. The search for the nearest neighbors was repeated for approximately 117 million non-water pixels within the LandWeb study area where the Landsat spectral data were available in the years 1990, 2000, and 2010 as well as for the dateless prediction. Imputation of the forest attributes was achieved by averaging canopy cover and height of the nearest neighbors or by taking the mode of the nearest neighbors in the case of the species associations.

Mapping the anthropogenic footprint

An objective of the LandWeb project was to develop a “sandbox” landscape for carrying out modelling exercises in the absence of anthropogenic disturbance. Toward this goal, we mapped out the cumulative anthropogenic footprint for the LandWeb study area *circa* 2010 and developed a kNN model that used only climate and elevation as predictor variables. We acquired several spatial layers for mapping the anthropogenic footprint in the LandWeb study area. The Boreal Ecosystem Anthropogenic Disturbance layer from 2010 was used for mapping cut blocks, non-road linear features (seismic lines, pipelines, railways, transmission lines), mines, and energy-related infrastructure (Pasher et al. 2013). A national road network inventory layer was acquired for the study area from Statistics Canada. A national agricultural inventory layer from 2011 was acquired for the study area from Agriculture and Agri-Foods Canada. Finally, we used the Stable nighttime lights product derived from the Defense Meteorological Satellite Program for mapping urban areas in the study area. Digital numbers of the stable nighttime lights layer greater than 50 were used to identify urban areas (Milesi et al. 2003). We chose the year 2010 as the base year because it was the latest year in the time series that is most likely to represent cumulative anthropogenic disturbance in the study area. The total anthropogenic footprint in the study area was estimated to be 17.4 Mha or 8.3% of the study area (Table 4). The combined footprint from all the sources listed in Table 4 was used to generate a spatial anthropogenic footprint mask at a 100 m (1 ha) pixel size (Figure 3). The largest contributing source was agriculture, accounting for more than half (53.3%) of the total anthropogenic footprint (Table 4).

Table 4. Sources contributing to the anthropogenic footprint in the LandWeb study area.

Source	Area (ha)	Percentage of footprint (%)
Agriculture ¹	9,259,863	53.3
Roads ^{2,3*}	4,114,180	23.7
Cut blocks ²	3,120,521	18.0
Urban ⁴	695,588	4.0
Mines ²	104,458	0.6
Oil and gas, including well sites ^{2,4}	83,992	0.4
Total	17,378,602 ha	100 %

* The area of all linear features was calculated by intersection with 100 m (1 ha) cells.

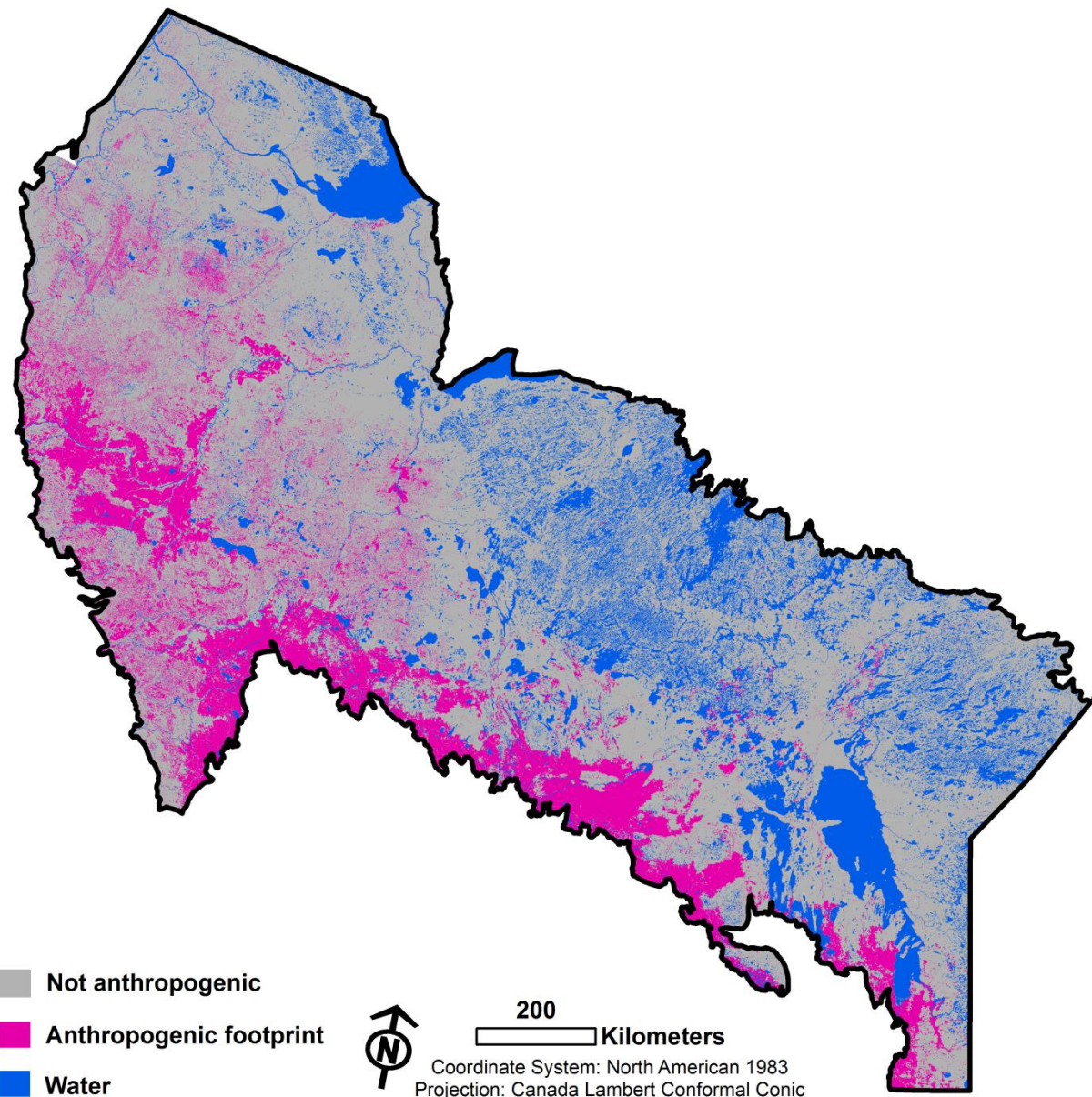
¹ Data source: Agriculture and Agri-Food Canada 2011

² Data source: http://ec.gc.ca/data_donnees/STB-DGST/002/BEAD_DATA LAYERS.zip

³ Data source: http://www12.statcan.gc.ca/census-recensement/2011geo/RNF-FRR/files-fichiers/grnf000r10a_e.zip

⁴ Data source: <http://ngdc.noaa.gov/eog/dmsp/downloadV4composites.html>

Figure 3. Extent of anthropogenic footprint across the LandWeb study area.



Filling the anthropogenic footprint

We mapped and filled any pixel identified as anthropogenic using a two-step process. First, spatial filtering of the predictions was undertaken by expanding the anthropogenic footprint by 1 pixel then shrinking it by 2 pixels. This process removed the majority of roads and smaller anthropogenic features. We then filled anthropogenic features 25 pixels (hectares) or smaller with the average of the neighbors in the case of height and canopy cover or the mode of the neighboring species associations. All remaining anthropogenic features were filled with the prediction of the kNN model trained on climate and elevation. Data gaps from the best available pixel method and ties that emerged from the voting for predicted species associations were filled

in the same way in order to provide a wall-to-wall estimate of the species associations within the LandWeb study area.

Creating a common vegetation mask

Codes were established for vegetation types (Table 2): forested (any value less than 200); vegetated, non-forested (240); and non-vegetated (230). These codes were derived from analysis of NDVI values across all decades. If NDVI exceeded 0.7 in any decade (1990, 2000, and 2010), then the pixel was considered forested. If NDVI was below 0.4 for all decades, then the pixel was considered non-vegetated. All remaining pixels ($0.4 < \text{NDVI} < 0.7$) were classified as vegetated, non-forested. There were 269,807 pixels for which a spectral value was not available in any decade, so without better information these pixels were assumed to be forested. For infilling the 1990 attributes, a nibble was performed on the anthropogenic footprint to remove most roads and linear features in the forest-vegetation mask. Any remaining anthropogenic features were classified as forested. Additionally, Chernozem soils identified in the Soil Landscapes of Canada database Version 3.2 (<http://sis.agr.gc.ca/cansis/nsdb/slcl/index.html>) were classified as vegetated. The final vegetation mask is shown in Figure 4.

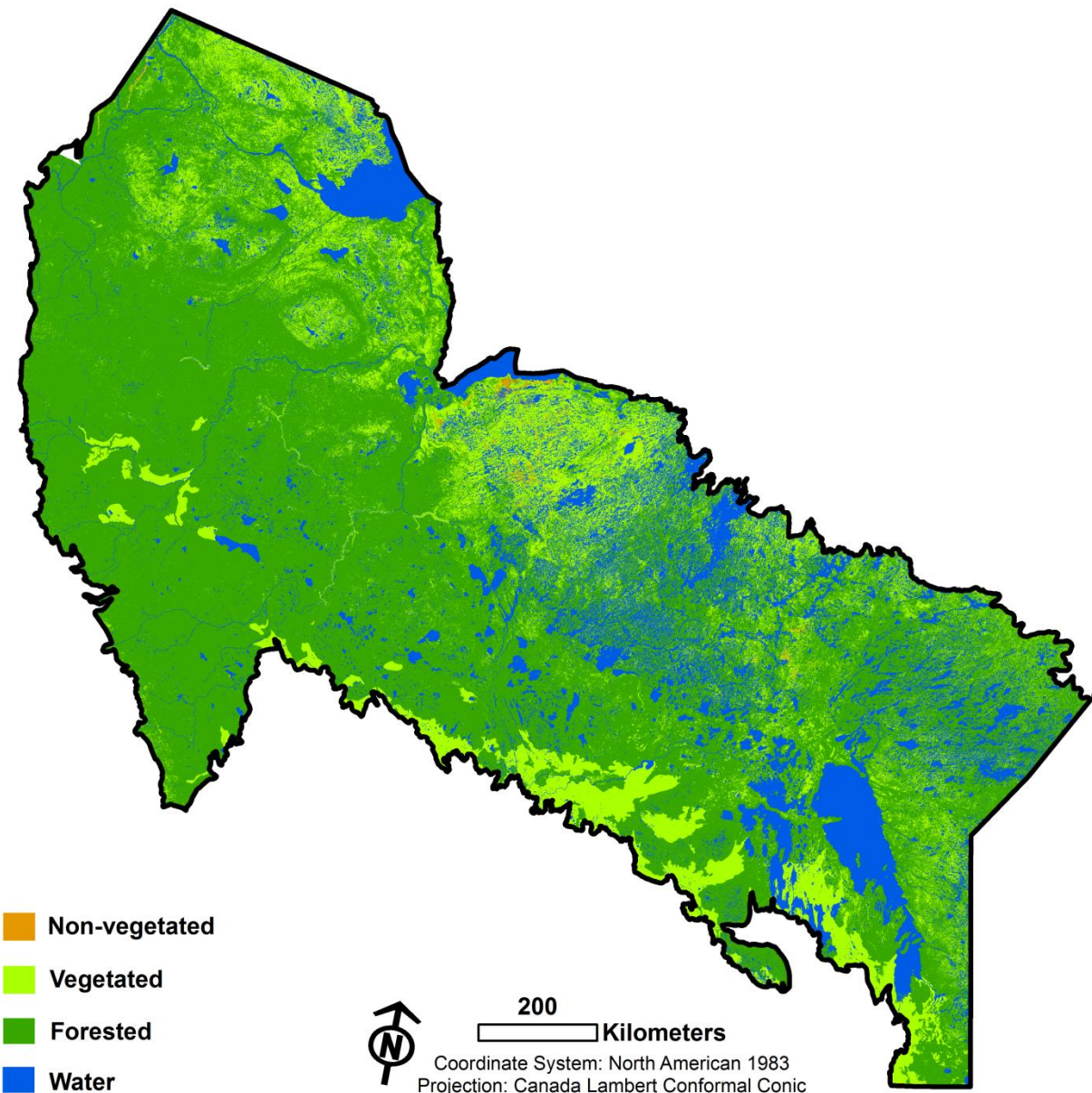
Accuracy Statements for LandWeb Data Layers

The output data layers are appended to this report for visual representation. The output data layers (height, canopy cover, and species association) were produced from the kNN imputation for the years 1990, 2000, and 2010. Each of these data layers are stand-alone products that can be used in conjunction with the filled attribute layers to derive the desirable landscape modelling conditions. In this section we provide accuracy assessments of the LandWeb output data layers.

Height and canopy cover layers

The accuracy of height and canopy cover variables was assessed using cross-validation and reported in terms of root mean squared difference (RMSD). The accuracy and number of training-validation samples for height and canopy cover for the three predicted decades are summarized in Table 5. CASFRI training samples were constrained by 3 km minimum distance to account for autocorrelation. As a result, the percentage of total CASFRI training samples ranged from 18.3% to 29.3% for height and 18.1% to 27.1% for canopy cover. Moreover, the number of CASFRI records available varied by decade with 2000 having the largest number of records and 2010 having the fewest number of records. Height accuracy ranged between 4.2 m in 2010 to 6.7 m in 1990. Canopy cover accuracy ranged from 20.1% in 2010 to 21.7% in 1990.

Figure 4. Classification of non-vegetated, vegetated, and forested pixels across the LandWeb study area.



Species association layers

The accuracy of the species association layers was assessed using cross-validation and reported in terms of an error matrix for all decades combined. User's accuracy ranged from 11% for pure white spruce (44) to 84% for pure deciduous (11). Producer's accuracy ranged from 22% for deciduous-Pinus (31) to 63% for pure deciduous (11). Across all classes, the overall accuracy was 49% (Table 6). When the species associations were collapsed by leading species, overall accuracy increased to 72% (Table 7).

Table 5. Summary of root mean squared difference (RMSD) for height (m) and canopy cover (%) during the four predicted time periods and the number of CASFRI training and validation samples used in cross-validation.

Variable	Decade	RMSD	Training Samples (%)	Validation Samples (%)
Height (m)	1990	6.7	2,766 (22.9)	9,329 (77.1)
	2000	6.5	3,469 (18.3)	15,524 (81.7)
	2010	4.2	509 (29.3)	1,227 (70.7)
Canopy cover (%)	1990	21.7	1,963 (24.9)	5,931 (75.1)
	2000	21.0	3,423 (18.1)	15,509 (81.9)
	2010	20.1	537 (27.1)	1,448 (72.9)

Table 6. Species association error matrix for all decades combined. Species association codes as in Table 2.

Mapped	Reference	11	14	22	23	26	31	32	33	34	41	42	43	44	User's accuracy
11	4295	416	38	3	119	185	1	10	3	48	4	1	13	83.63	
14	1405	705	31	1	73	123	4	4	5	147	6	9	27	27.76	
22	62	22	1136	100	547	62	50	68	15	14	9	5	10	54.10	
23	13	15	395	542	98	78	290	32	21	16	12	13	6	35.40	
26	200	49	618	47	1815	82	41	44	13	21	15	5	6	61.40	
31	344	142	55	19	65	304	30	12	23	51	8	18	7	28.20	
32	9	6	83	107	51	59	313	66	28	11	9	15	4	41.13	
33	76	6	128	47	69	79	146	268	22	15	11	10	8	30.28	
34	37	35	76	66	66	141	180	48	177	61	18	65	16	17.95	
41	230	221	129	27	126	126	41	22	25	422	33	22	55	28.53	
42	25	21	58	20	45	15	6	10	4	36	52	5	12	16.83	
43	74	50	43	30	27	85	48	13	50	56	13	80	11	13.79	
44	85	60	78	18	66	44	16	12	10	103	17	9	65	11.15	
Producer's accuracy	62.65	40.33	39.61	52.78	57.31	21.98	26.84	44.01	44.70	42.16	25.12	31.13	27.08	Overall Accuracy 48.62	

Table 7. Leading species error matrix for all decades combined.

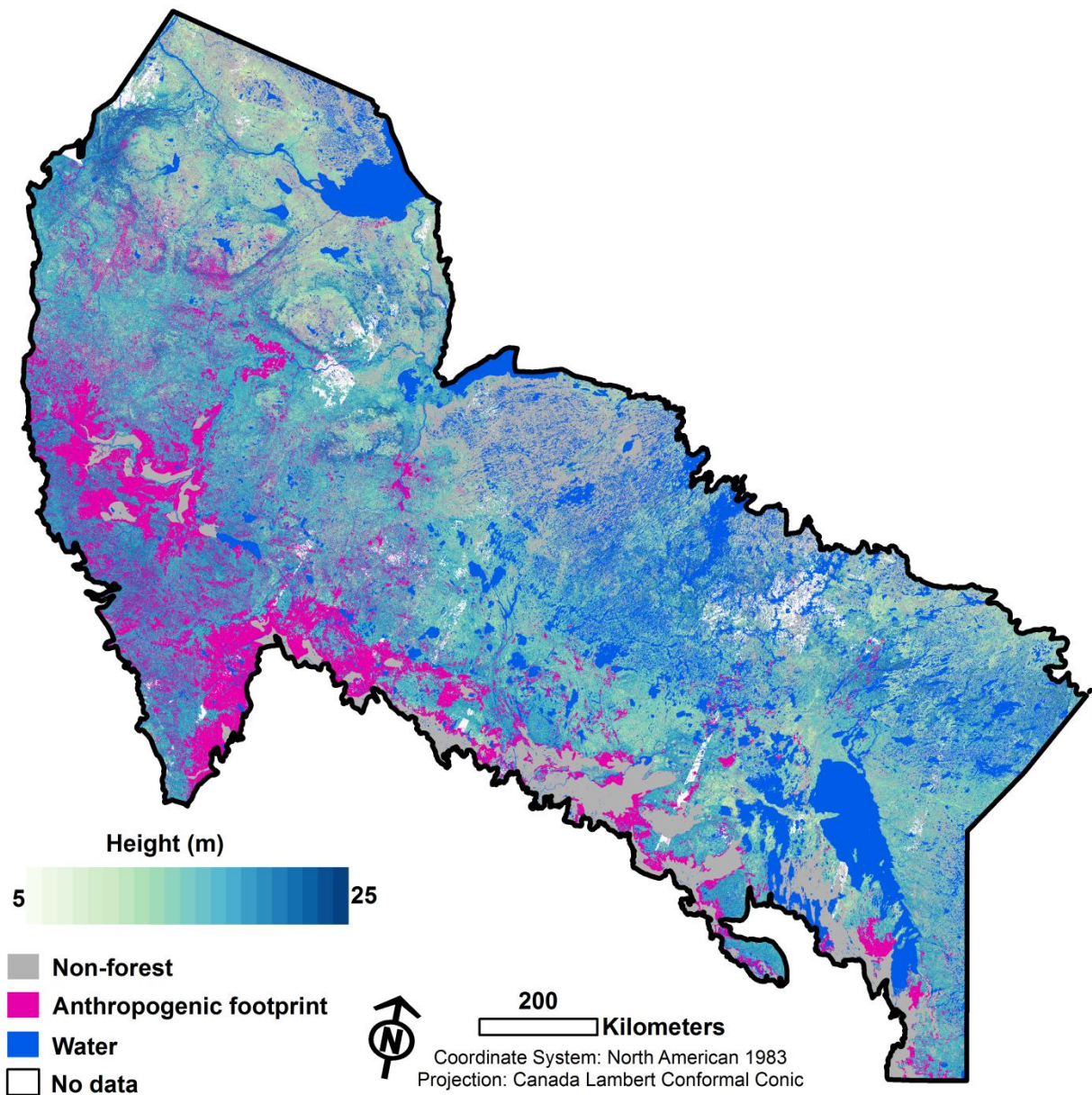
Mapped	Reference Deciduous	P. mariana	Pinus spp.	P. glauca	User's Accuracy
Deciduous	6821	265	335	255	88.86
P. mariana	361	5298	796	132	80.43
Pinus spp.	655	832	1896	327	51.11
P. glauca	766	667	527	991	33.58
Producer's Accuracy	79.29	75.02	53.35	59.34	Overall Accuracy 71.72

References

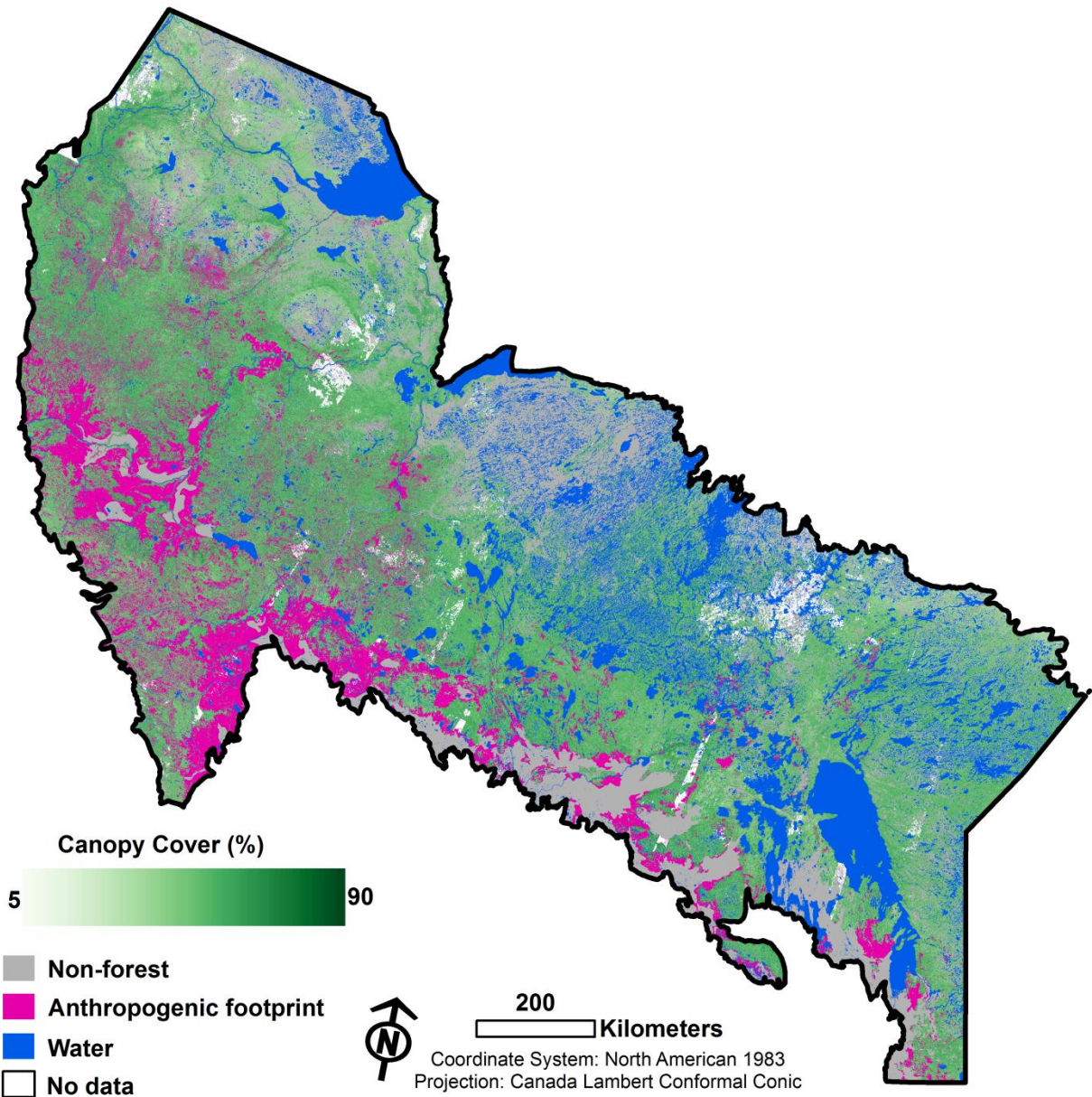
- Beaudoin, A., Bernier, P.Y., Guindon, L., Villemaire, P., Guo, X.J., Stinson, G., Bergeron, T., Magnussen, S., and Hall, R.J. 2014. Mapping attributes of Canada's forests at moderate resolution through kNN and MODIS imagery. Canadian Journal of Forest Research 44: 521-532.
- Crookston, N.L., and Finley, A.O. 2008. yaImpute: an R package for kNN imputation. Journal of Statistical Software 23: 1-16.
- Cumming, S.G., Drever, R., Houle, M., Cosco, J., Racine, P., Bayne, E., and Schmiegelow, K.A. 2015. A gap analysis of tree species representation in the protected areas of the Canadian boreal forest: applying a new assemblage of digital Forest Resource Inventory data. Canadian Journal of Forest Research 45: 163-173.
- Ecological Stratification Working Group (ESWG). 1996. National Ecological Framework for Canada. Centre for Land and Biological Resources Research, Research Branch, Agriculture and Agri Foods Canada, Ottawa, Ont., and State of Environment Directorate, Environment Canada, Ottawa, Ont. Available: http://sis.agr.gc.ca/cansis/publications/ecostrat/cad_report.pdf.
- Hamann, A., Wang, T., Spittlehouse, D.L., and Murdock, T.Q. 2013. A comprehensive, high-resolution database of historical and projected climate surfaces for western North America. Bulletin of the American Meteorological Society 94: 1307-1309.
- Masek, J.G., Vermote, E.F., Saleous N.E., Wolfe, R., Hall, F.G., Huemmrich, K.F., Gao, F., Kutler, J., and Lim, T-K. 2006. A Landsat surface reflectance dataset for North America, 1990–2000. IEEE Geoscience and Remote Sensing Letters 3: 68-72.
- McRoberts, R.E., Nelson, M.D., and Wendt, D.G. 2002. Stratified estimation of forest area using satellite imagery, inventory data, and the k-Nearest Neighbors technique. Remote Sensing of Environment 82: 457-468.
- Milesi, C., Elvidge, C.D., Nemani, R.R., and Running, S.W. 2003. Assessing the impact of urban land development on net primary productivity in the southeastern United States. Remote Sensing of Environment 86: 401-410.
- Pasher, J., Seed, E., and Duffe, J. 2013. Development of boreal ecosystem anthropogenic disturbance layers for Canada based on 2008 to 2010 Landsat imagery. Canadian Journal of Remote Sensing 39: 42-58.
- White, J.C., Wulder, M.A., Hobart, G.W., Luther, J.E., Hermosilla, T., Griffiths, P., Coops, N.C., Hall, R.J., Hostert, P., Dyk, A., and Guindon, L. 2014. Pixel-based image compositing for large-area dense time series applications and science. Canadian Journal of Remote Sensing 40: 192-212.

Wulder, M.A., Dechka, J.A., Gillis, M.A., Luther, J.E., Hall, R.J., Beaudoin, A., and Franklin, S.E. 2003. Operational mapping of the land cover of the forested area of Canada with Landsat data: EOSD land cover program. *The Forestry Chronicle* 79:1075-1083.

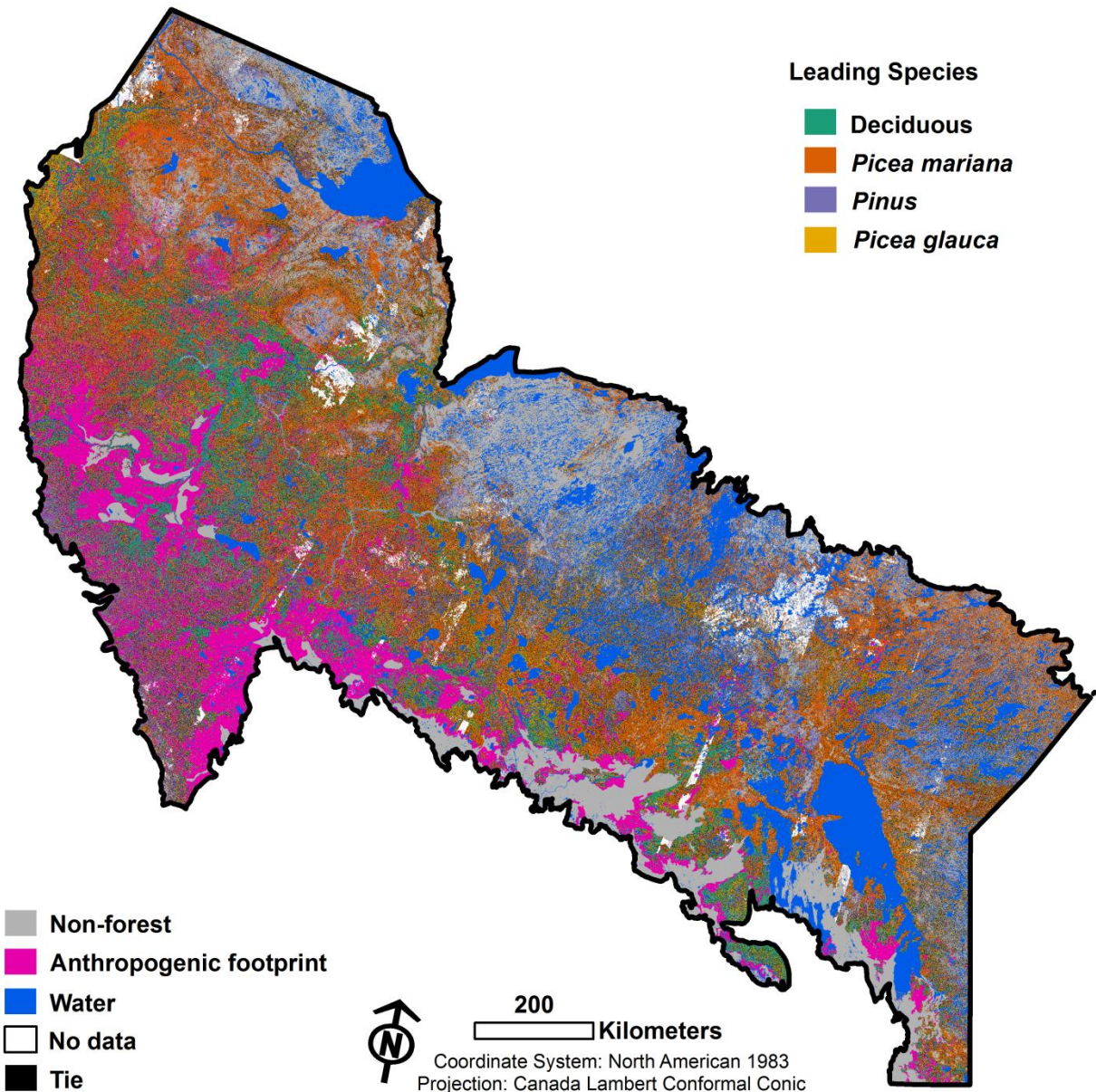
1990 Height (m)



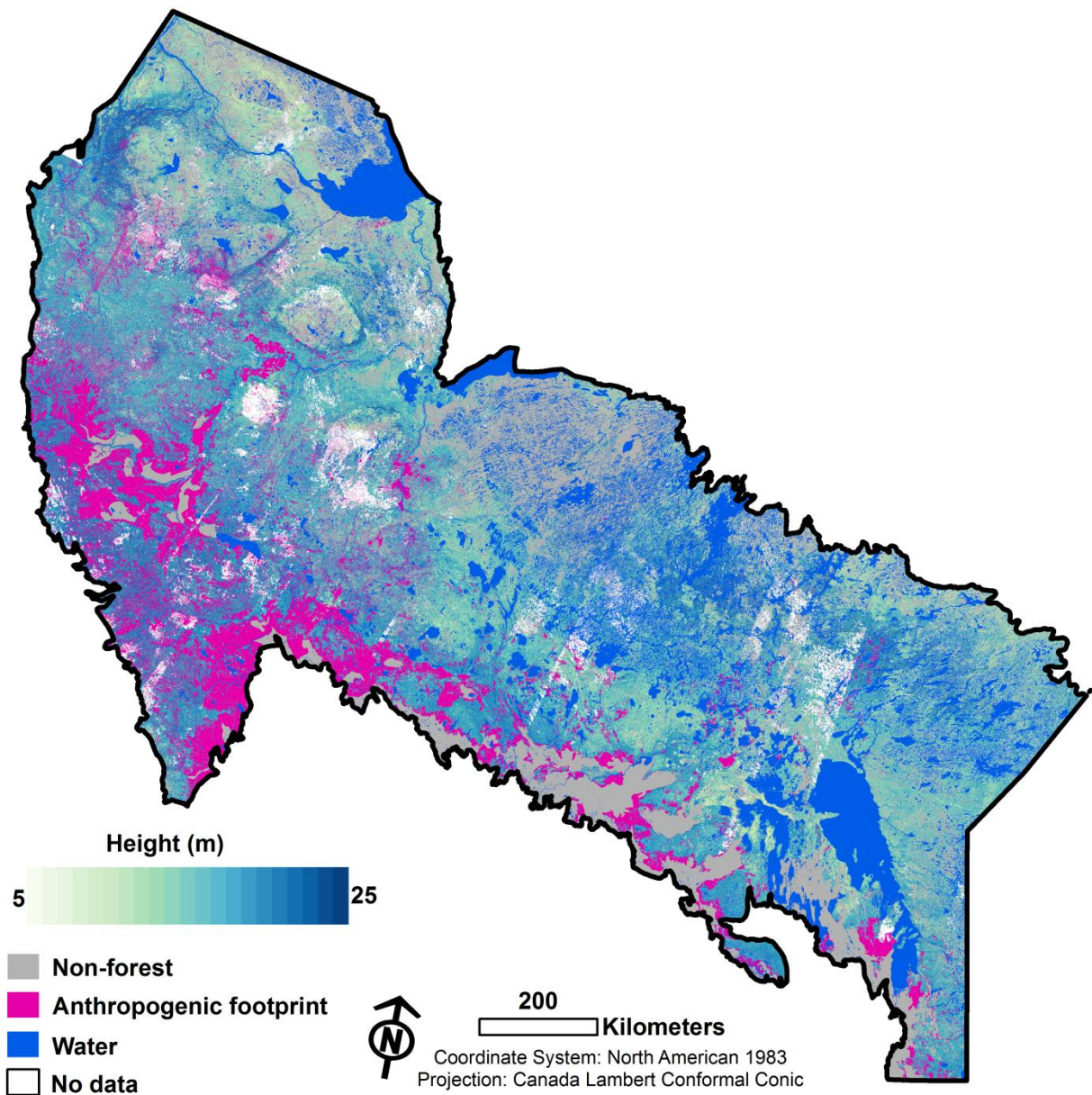
1990 Canopy Cover (%)



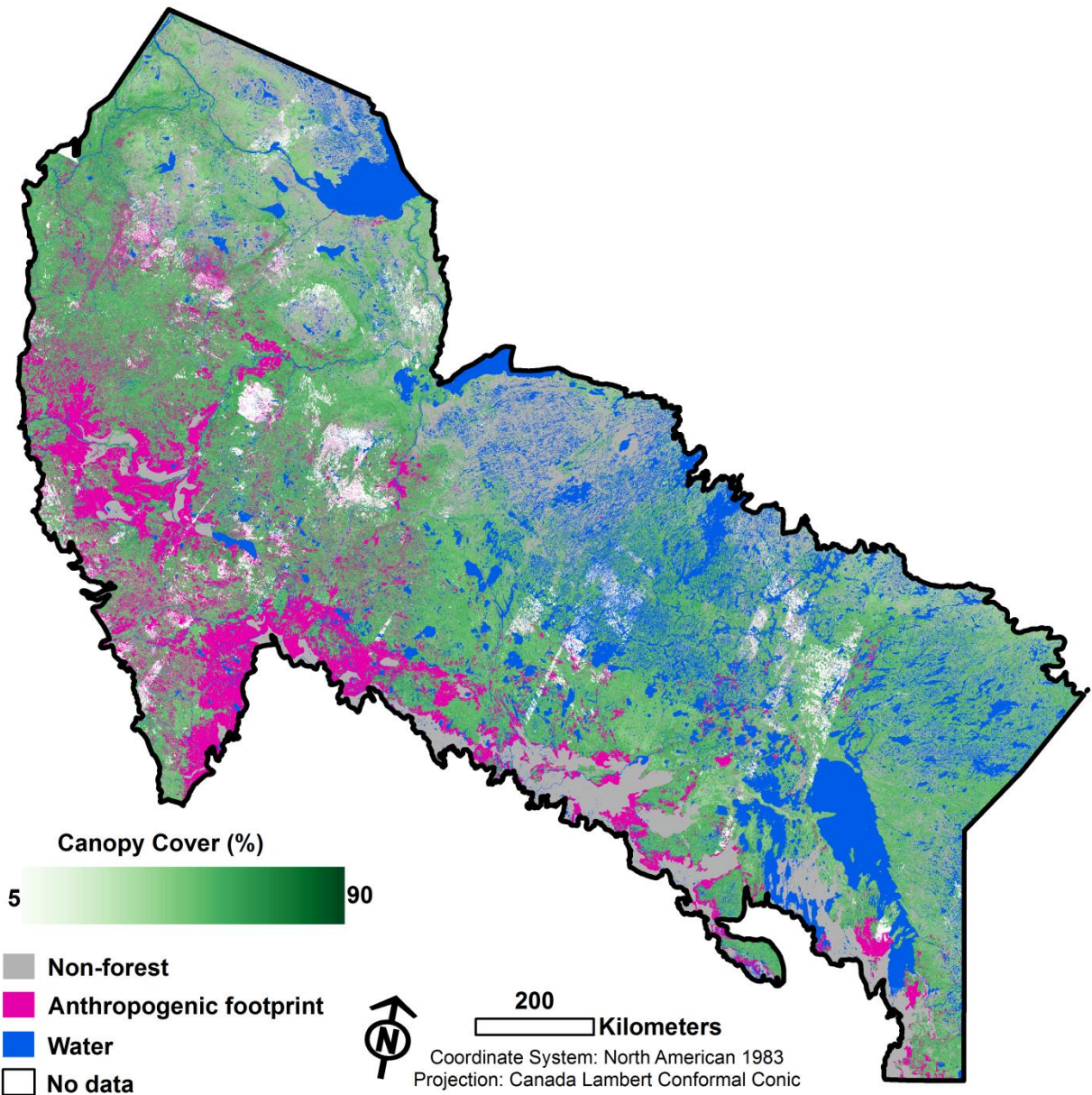
1990 Species Association



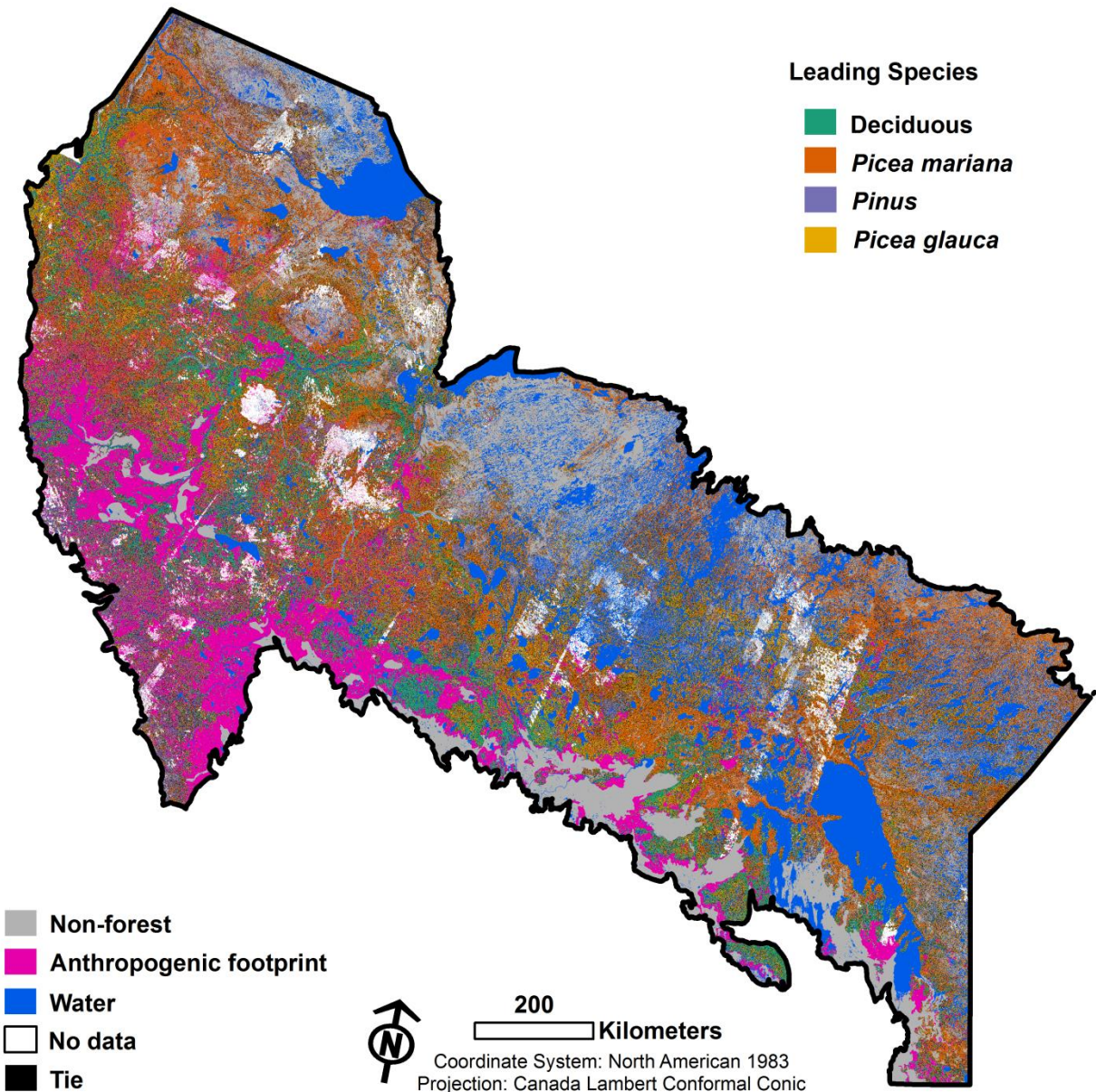
2000 Height (m)



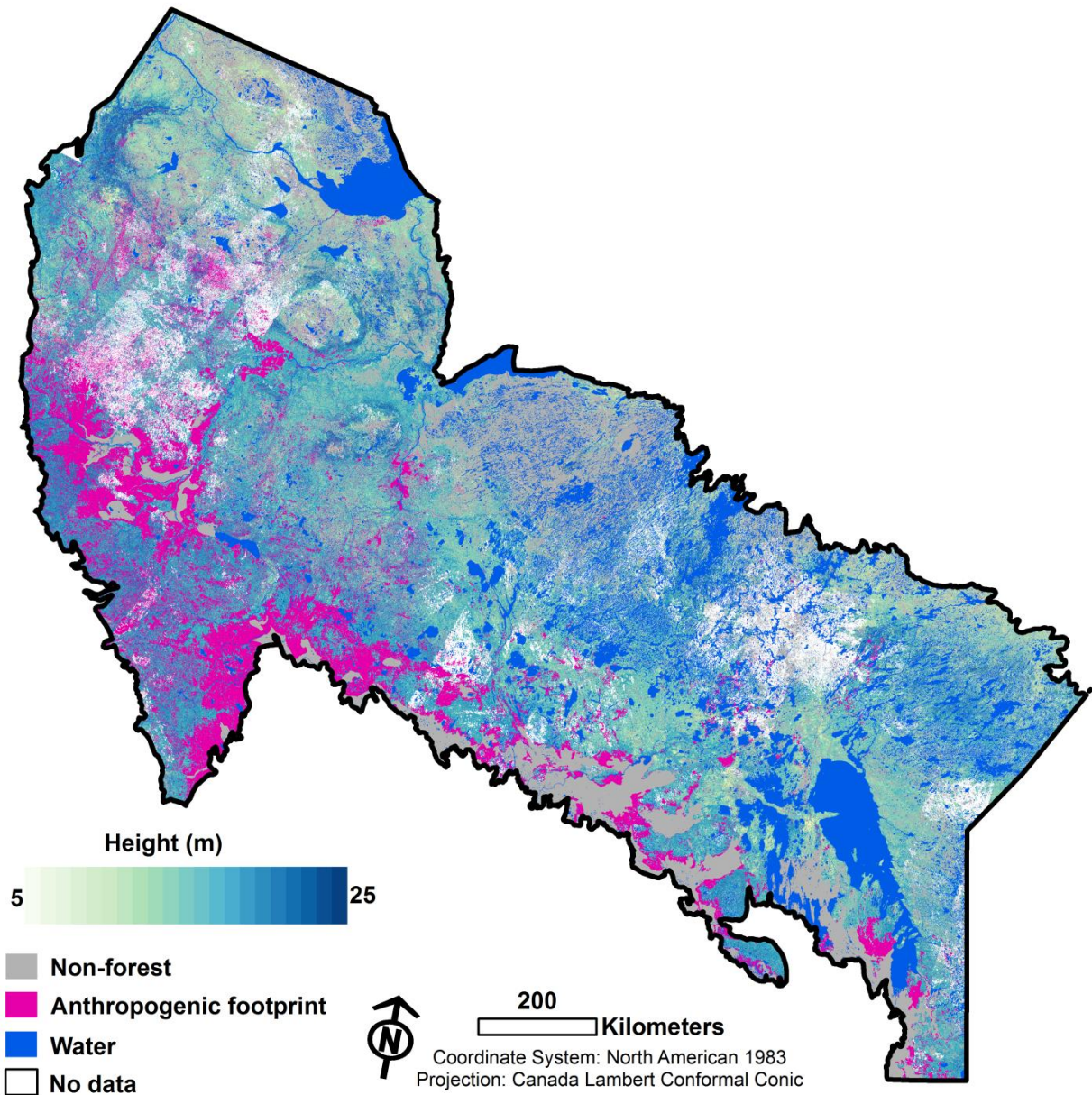
2000 Canopy Cover (%)



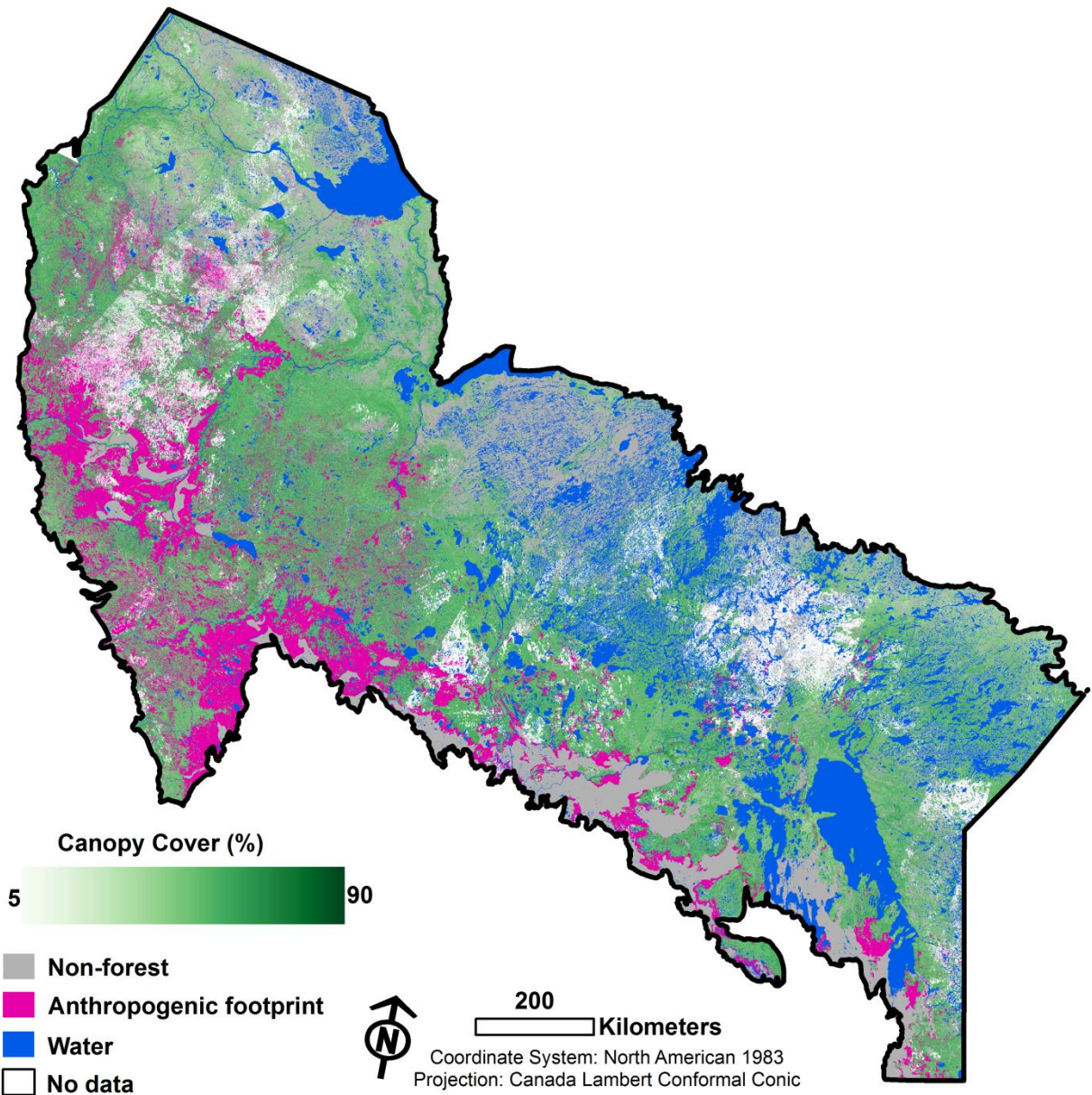
2000 Species Association



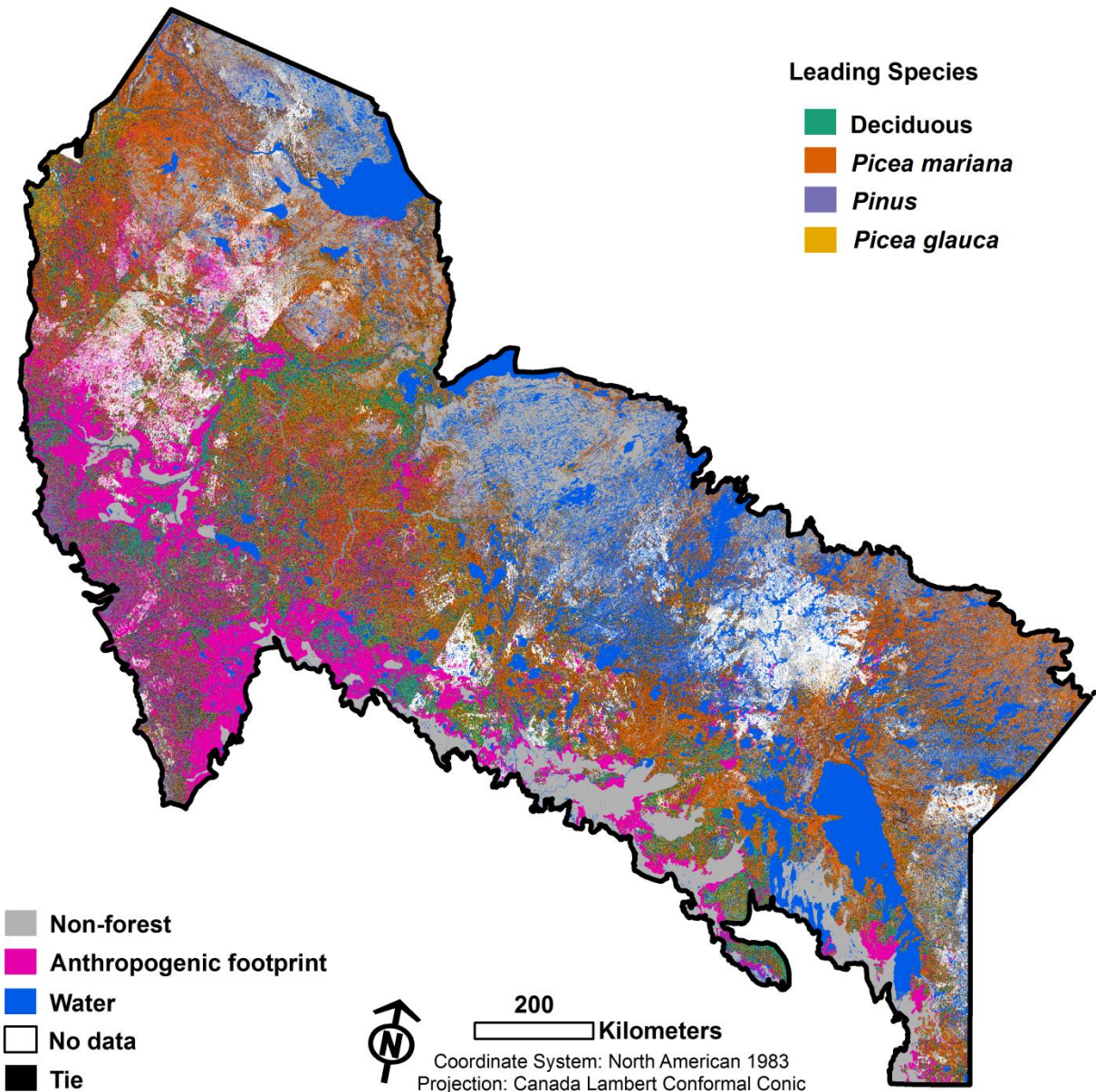
2010 Height (m)



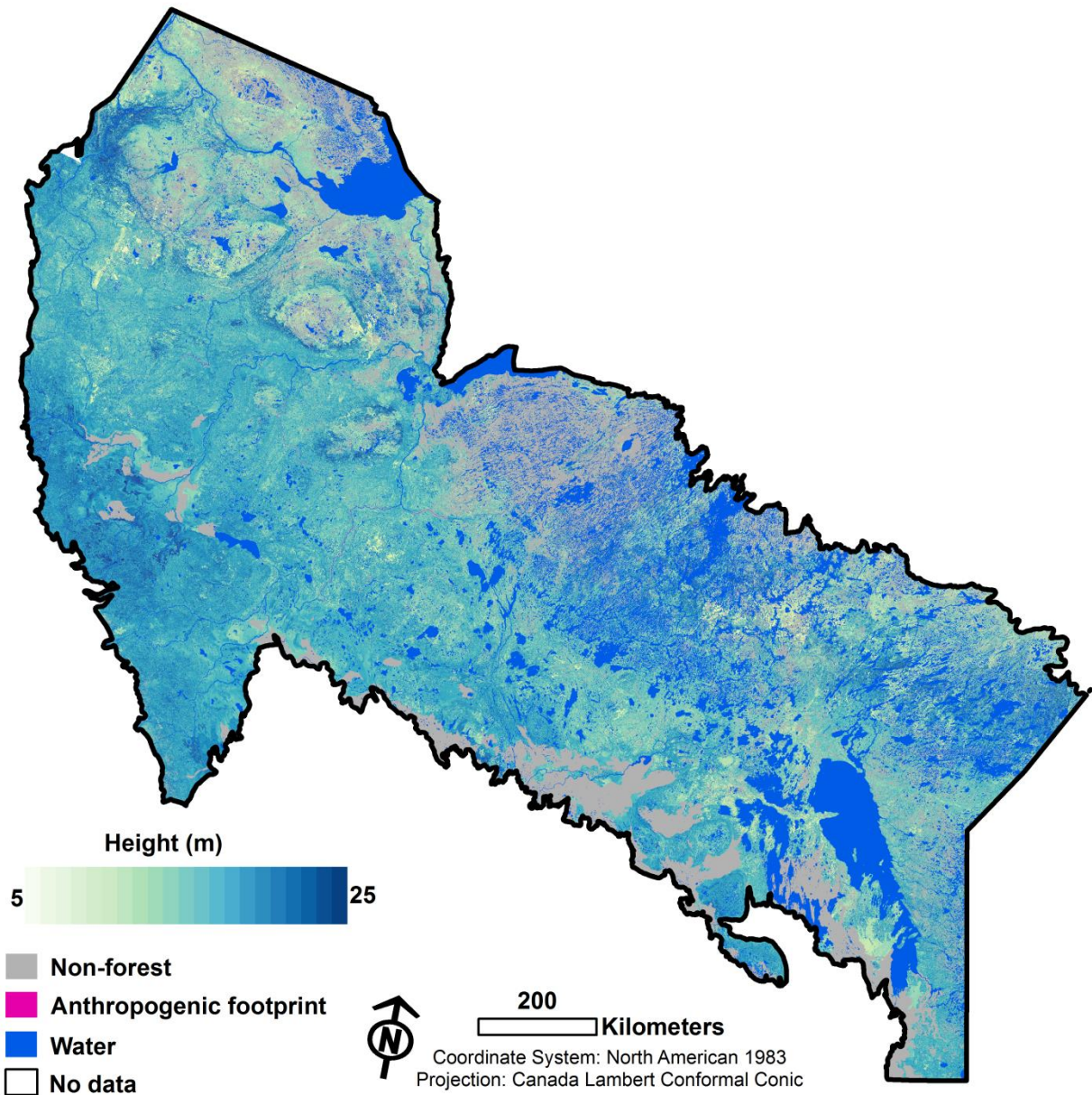
2010 Canopy Cover (%)



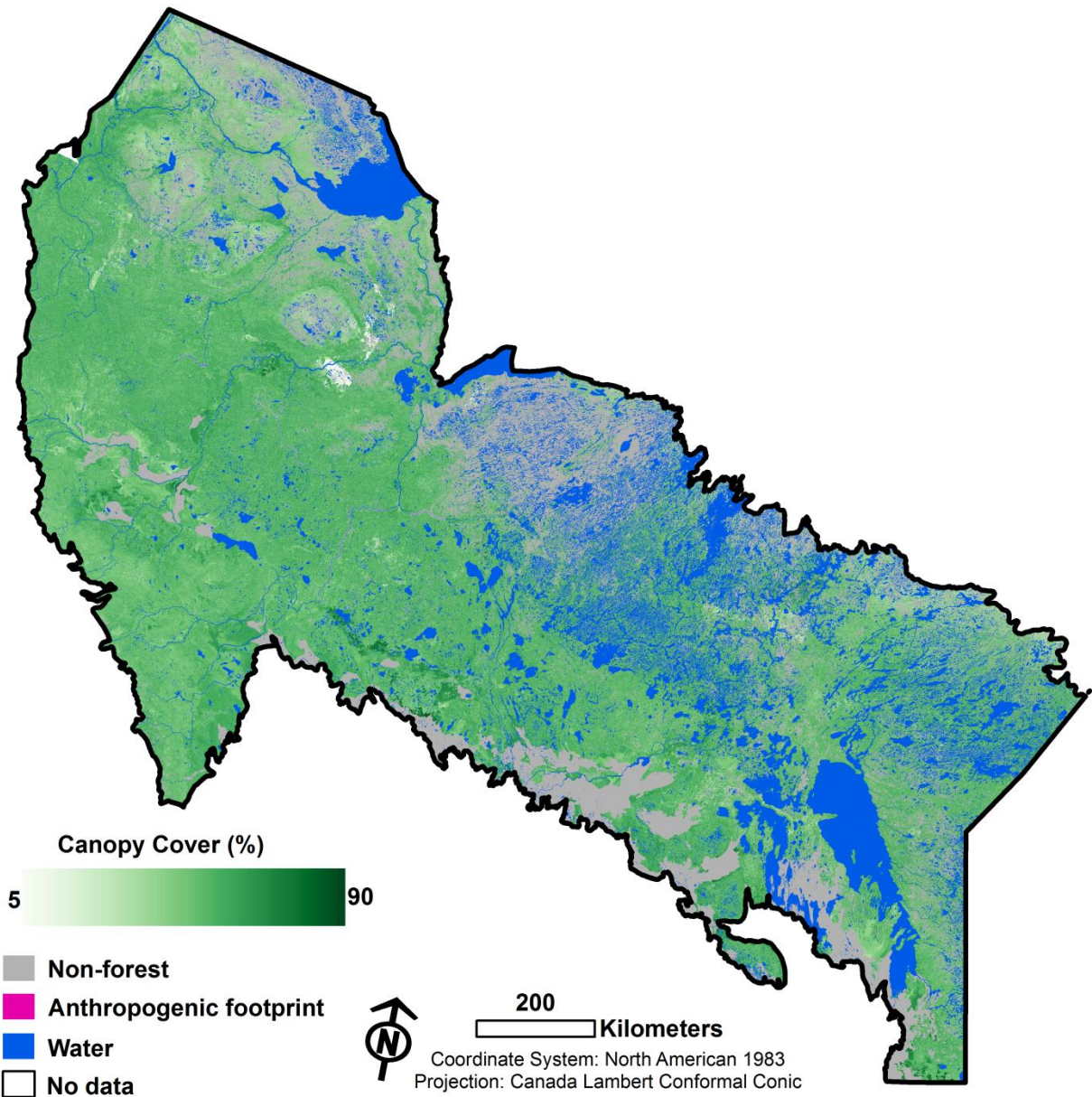
2010 Species Association



Filled Height (m)



Filled Canopy Cover (%)



Filled Species Association

